



OPEN Unraveling the role of gut microbiota by fecal microbiota transplantation in rat model of kidney stone disease

Sittiphong Hunthai¹, Manint Usawachintachit², Mana Taweewisit³,
 Monpichar Srisa-Art⁴, Weerapat Anegkamol¹, Piyaratana Tosukhowong¹,
 Pakkapon Rattanachaisit¹, Natthaya Chuaypen¹ & Thasinas Dissayabutra¹✉

Emerging research on the microbiome highlights the significant role of gut health in the development of kidney stones, indicating that an imbalance in gut bacteria or dysbiosis can influence the formation of stones by altering oxalate metabolism and urinary metabolite profiles. In particular, the overabundance of specific bacteria such as *Enterococcus* and *Oxalobacter* spp., which are known to affect oxalate absorption, is observed in patients with urolithiasis. This study investigates the effects of gut dysbiosis on urolithiasis through fecal microbiota transplantation (FMT) from patients to rats and its impact on urinary mineral excretion and stone formation. Fecal samples from eight patients with calcium oxalate stones and ten healthy volunteers were collected to assess the gut microbiome. These samples were then transplanted to antibiotic-pretreated Wistar rats for a duration of four weeks. After transplantation, we evaluated changes in the fecal gut microbiome profile, urinary mineral excretion rates, and expression levels of intestinal *zonula occluden-1 (ZO-1)*, *SLC26A6* and renal *NF-κB*. In humans, patients with urolithiasis exhibited increased urinary calcium and oxalate levels, along with decreased citrate excretion and increased urinary supersaturation index. The fecal microbiota showed a notable abundance of *Bacteroidota*. In rodents, urolithiasis-FMT rats showed urinary disturbances similar to patients, including elevated pH, oxalate level, and supersaturation index, despite negative renal pathology. In addition, a slight elevation in the expression of renal *NF-κB*, a significant intestinal *SLC26A6*, and a reduction in *ZO-1* expression were observed. The gut microbiome of urolithiasis-FMT rats showed an increased abundance of *Bacteroidota*, particularly *Muribaculaceae*, compared to their healthy FMT counterparts. In conclusion, the consistent overabundance of *Bacteroidota* in both urolithiasis patients and urolithiasis-FMT rats is related to altered intestinal barrier function, hyperoxaluria, and renal inflammation. These findings suggest that gut dysbiosis, characterized by an overgrowth of *Bacteroidota*, plays a crucial role in the pathogenesis of calcium oxalate urolithiasis, underscoring the potential of targeting the gut microbiota as a therapeutic strategy.

Keywords Urolithiasis, Gut microbiota, Fecal microbiota transplantation, Oxalate, Gut leakage

Urolithiasis, a major global health issue, affects a wide range of populations regardless of demographics or geography¹, with an estimated 10–15% of the global population experiencing this condition at least once in their life². The origins of urolithiasis are complex and multifaceted, involving a combination of genetic predispositions, diet practices, fluid consumption, and underlying health conditions such as obesity, diabetes, and hypertension. Stone formation is mainly due to the supersaturation of the urine with minerals like calcium, oxalate, phosphate, urate, and cystine³, a process influenced by urinary pH and the balance between crystallisation inhibitors and promoters.

Recent breakthroughs in microbiome research have highlighted the significant role of the gut microbiota in the pathogenesis of kidney stones, marking a pivotal shift in our understanding and management strategies

¹Metabolic Disease in Gastrointestinal and Urinary System Research Unit, Department of Biochemistry, Faculty of Medicine, Chulalongkorn University, Bangkok 10330, Thailand. ²Division of Urology, Department of Surgery, Faculty of Medicine, Chulalongkorn University, Bangkok 10330, Thailand. ³Department of Pathology, Faculty of Medicine, Chulalongkorn University, Bangkok 10330, Thailand. ⁴Department of Chemistry, Faculty of Science, Chulalongkorn University, Bangkok 10330, Thailand. ✉email: thasinas@chula.md

for urolithiasis. Emerging studies suggest that gut dysbiosis, or the imbalance of the gut microbiota, could substantially impact the risk and development of kidney stones through mechanisms such as modulation of urinary metabolites, changes in intestinal oxalate metabolism, and systemic inflammatory response⁴. In particular, bacteria such as *Oxalobacter* spp., especially *O. formigenes*, known for their ability to degrade oxalate, could reduce oxalate absorption and lower the risk of stone formation^{5,6}. However, recent evidence suggests that supplementing with *O. formigenes* may not effectively lower urinary oxalate levels or prevent stone formation^{7–9}. Furthermore, a phase III clinical trial focussing on children with primary hyperoxaluria found no significant change in plasma oxalate levels after a year of treatment with *O. formigenes*, further questioned the efficacy of such intervention¹⁰.

Rather than *Oxalobacter*, other gut microbiota can exert wider effects that contribute to stone pathogenesis, including modulation of the host's immune system, intestinal permeability, and inflammatory pathways. Gut bacteria such as *Lactobacillus*, *Bifidobacterium*, *Eubacterium*, and *Enterococcus faecalis* have been implicated in the processes of oxalate absorption and stone formation¹¹. Previous studies revealed the oxalate degrading capacity of *B. animalis* subsp. *Lactis*, *E. lentum*, *E. faecalis*, *B. lactis* and *L. plantarum* in vitro, particularly due to the presence of the *oxalate decarboxylase* gene¹².

In patients with stone disease, patterns of gut dysbiosis, characterized by varying abundances of specific microbial genera, have been identified. Increased abundance of *Bacteroidota*, *Escherichia-Shigella* and less abundance of *Prevotella_9* commonly present in patients with urolithiasis^{13,14}. These anomalies suggest a complex interplay between gut microbial composition and urolithiasis, which is not limited to exclusive degradation of oxalates. Interestingly, fecal transplantation studies, such as the one in which the microbiota of Zucker lean mice were transferred to germ-free mice, have shown potential to reduce urinary excretion of calcium, oxalate, and alter intestinal pH levels, pointing towards gut dysbiosis as a contributing factor to urolithiasis¹⁵. Despite the accumulation of evidence of an association between the gut microbiota and stone formation, the causality of this relationship remains to be fully elucidated.

The study is designed to investigate the gut microbial communities in patients with urolithiasis compared to healthy individuals. To further elucidate the pathophysiology of gut dysbiosis in calcium oxalate lithogenesis, we transplanted the fecal microbiota of urolithiasis patients into antibiotic-pretreated rats and contrasted these results with volunteer-FMT rats. We seek to uncover the specific role that gut dysbiosis plays in altering the intestinal gut barrier, urinary mineral excretion patterns, and renal inflammation.

Materials and methods

This research included cross-sectional studies on the human microbiome and experimental studies in animals.

Ethical declaration

The study involved the collection of urine and stool samples using anaerobic methods and was approved by the Institutional Review Board, Faculty of Medicine, Chulalongkorn University, Thailand (COA No. 0995/2022). The experiments were performed in accordance with the Declaration of Helsinki. Informed consent was obtained from all participants. The animal study protocol was approved by the Chulalongkorn University Animal Care and Use Committee of the Faculty of Medicine, Chulalongkorn University, Thailand (CU-ACUC No. 004/2565). All experiments were performed according to the IACUC and ARRIVE guidelines and regulations.

Human participants

In this study, eight patients with calcium oxalate urolithiasis received surgical treatment at the Chulalongkorn Hospital Urological Surgery Unit and ten healthy participants were included. Urine samples from the morning, first voiding spot urine samples were obtained to assess creatinine, calcium, and magnesium levels using electrochemiluminescence (COBAS C6000, Roche, USA) and to measure oxalate and citrate by capillary electrophoresis (P/ACETM MDQ, Beckman Coulter, USA). Fecal samples were also gathered using the AnaeroPouch - Anaero system (Mitsubishi Gas Chemical Co., Japan), from which a portion was treated to isolate DNA with a DNA/RNA shield (Zymo Research, USA) for subsequent sequencing.

16 S rRNA amplicon sequencing and analysis

To sequence 16s rRNA, the hypervariable V4 regions of the 16 S rRNA genes were amplified from DNA samples using 515 F (5'GTGCCAGCMGCCGCGTAA 3') and 806R (5'GGACTACHVGGGTWTCTAAT3') primers and 2X KAPA hot start ready mix. The PCR conditions included an initial denaturation at 94 °C for 3 min, followed by 25 cycles of 98 °C for 20 s, 55 °C for 30 s 72 °C for 30 s, and a final extension step at 72 °C for 5 min. The 16 S amplicons were purified using AMPure XP beads and indexed using the Nextera XT index kit, followed by 8 cycles of the aforementioned PCR condition. Finally, the PCR products were cleaned and pooled for cluster generation and 250 bp paired-end read sequencing on the Illumina MiSeq (Mod Gut Co., Ltd., Bangkok, Thailand).

The quality of the raw data was assessed using FastQC (v0.11.8) and MultiQC (v1.7). QIIME2 (version 2022.2) was applied to perform microbiome analysis. The adapter and preceding bases were trimmed at the 5' end of the reads using the q2-cutadapt plugin. Reads with expected errors (maxEE) higher than 3.0 were discarded, paired end reads were merged with an overlap of 25 nucleotides between forward and reverse reads, and chimeric sequences were filtered using the q2-dada2 plugin.

The taxonomic classifier was trained using the V4 sequence based on the naive Bayes classifier model using the q2-feature classifier plugin. Amplicon sequence variants (ASVs) were assigned for taxonomy based on the reference sequences of Sklearn method against the SILVA (version 138.1) 99% operational taxonomic units (OTUs). The unassigned mitochondria and chloroplast sequences were removed using the q2-taxa plugin. Calculations of the rarefaction curve, richness index diversity index, and Principal coordinate analysis (PCoA)

and permutational multivariate analysis of variance (PERMANOVA) based on the Bray-Curtis distance were generated using the vegan package of R4.0.3.

Human urinary supersaturation index was calculated using the following equation¹⁶:

$$AP_{CaOx} = \frac{2.7 \bullet \text{Calcium}^{0.84} \bullet \text{Oxalate}}{\text{Citrate}^{0.22} \bullet \text{Magnesium}^{0.12} \bullet \text{Volume}^{1.03}}$$

AP_{CaOx} : Approximate Estimation of the Ion Activity Product of calcium oxalate.

Fecal microbiota transplantation (FMT) in Wistar rats

Three-week-old male Wistar rats, sourced from Nomura Siam Co. LTD in Thailand underwent a one-week acclimatization period before being housed in normal showbox cages in the Animal Lab at the Faculty of Medicine, Chulalongkorn University. The laboratory environment was meticulously controlled, maintaining a temperature of 25 °C, relative humidity between 30 and 50%, and a consistent 12-hour light/dark cycle. Throughout the study, rats had unrestricted access to food and water. To initiate partial eradication of the gut microbiota, their drinking water was supplemented with a cocktail of antibiotics (ampicillin 1 g/L, ciprofloxacin 1 g/L, metronidazole 1 g/L, and vancomycin 0.5 g/L) for a duration of 7 days¹⁷. Following this phase, the rats were organized into two groups, each comprising six individuals. From week 0, systematic collections of blood, urine, and fecal samples were carried out for further analysis.

To create the fecal microbiota extract, we pooled 3 g of each fecal sample from urolithiasis into a urolithiasis-FMT mixture, and each sample from the volunteer into a healthy mixture of FMT, separately. Each sample was dissolved in 45 mL of 0.9% sodium chloride solution. The samples were then vigorously vortexed for 10 s and meticulously filtered three times through gauze, all under strict anaerobic conditions to preserve microbial integrity. Following filtration, the mixtures were centrifuged at 6,000 g for 15 min, allowing the collection of the clear supernatant¹⁸. The supernatant was then carefully combined with 20% glycerol, forming a protective medium for the microbial content, and subsequently stored at -20 °C for future analyses¹⁹.

During the experimental phase, the control group received an FMT solution derived from healthy individuals, while the urolithiasis group was administered FMT derived from patients with kidney stones. Each administration of FMT involved a 400 µL volume, administered by gavage twice weekly for a duration of four weeks. To simulate a high oxalate intake, sodium oxalate was incorporated into the drinking water of both groups at a concentration of 1% (w/w).

At the end of the experiment, the rats were placed in a metabolic cage for 24 h to collect the urine sample. Isoflurane was used as an anesthetic drug for blood collection from the retrobulbar vein before euthanasia using CO₂ inhalation, and intestinal fecal samples were harvested immediately after euthanization. Subsequently, the intestines and jejunum were meticulously harvested for further analysis. In our biochemical assessment, blood samples were analysed for calcium and magnesium levels, while urine samples were evaluated for concentrations of calcium, magnesium, oxalate, citrate, creatinine and urinary supersaturation index.

Urinary supersaturation index was calculated using the following equation¹⁶:

$$AP_{CaOx} = \frac{4067 \bullet \text{Calcium}^{0.93} \bullet \text{Oxalate}^{0.96}}{(\text{Citrate} + 0.015)^{0.60} \bullet \text{Magnesium}^{0.55} \bullet \text{Volume}^{0.99}}$$

For histological and genetic analyses, the intestines and kidneys were sectioned into two parts. The first section was forwarded to the Department of Pathology of the Faculty of Medicine, Chulalongkorn University, for detailed histopathological examination. The second section was RNA extraction using TRIzol LS reagent to facilitate RT-PCR assays. These assays were specifically designed to quantify the expression levels of intestinal zonula occluden-1 (ZO-1) and the oxalate transporter, Solute Carrier Family 26 Member 6 (SLC26A6), which offers insight into the molecular impact of our experimental interventions.

Fecal microbiota analyses

DNA extractions from bacterial feces were performed in both human and animal models using the Quick-DNATM Fecal/Soil Microbe Microprep Kit. The DNA extract was forwarded to ModGut Co., Ltd. (Thailand) for a comprehensive analysis of the fecal microbiota present in participants and animal models alike. To analyze the biological data of the 16 S rRNA (V3-V4 region), we employed QIIME software (Quantitative Insights into Microbial Ecology) software, a powerful tool for microbial community analysis. Sequences had been classified into various operational taxonomic units (OTUs), providing a detailed framework for understanding the diversity of microbials. To evaluate the diversity within the microbial population, we calculated the relative abundance using Shannon's index.

Histopathology analyses

Kidney and jejunum samples were meticulously sectioned transversely, then carefully placed on cassettes and submerged in 10% neutral buffer formalin to ensure their preservation. The Department of Pathology of the Faculty of Medicine, Chulalongkorn University carried out the tissue staining process. The jejunum sections were stained with hematoxylin and eosin (H&E) and further analyzed through immunohistochemistry to detect ZO-1 expression.

For the assessment of histopathological changes in the kidneys of animal models, crystal deposits were examined in three distinct regions: the cortex, the cortical medullary junction, and the tip of the papillary²¹. This examination was conducted using a polarizing microscope at a magnification of X400. In a similar vein,

jejunum sections were scrutinized under a microscope to evaluate ZO-1 staining, providing insight into the integrity of the intestinal barrier²². A pathologist was responsible for the scoring of these observations, ensuring a thorough and expert analysis of the histopathological features presented in both the kidney and intestinal samples of animal models.

Gene expression

Gene expression levels were accurately quantified using the quantitative polymerase chain reaction (qPCR) technique, employing the state-of-the-art QuantStudio™ 5 Real-Time PCR System. Complementary DNA (cDNA), synthesized from jejunum samples using the RevertAid First Strand cDNA Synthesis Kit, served as the template for measuring the expression of key genes: Zonula occluden-1 (*ZO-1*)²³, Solute carrier family 26, Member 6 (*SLC26A6*)²⁴ in the jejunum and the Nuclear Factor Kappa B subunit 1 gene (*NF-κB*)²⁵ in the kidney. The glyceraldehyde-3-phosphate dehydrogenase (*GAPDH*) gene was used as the reference gene²³. CT values obtained from qPCR were utilized to calculate the gene expression levels using the $2^{-\Delta\Delta Cq}$ method. This analysis could provide information on the relative expression levels of target genes compared to the housekeeping gene.

Statistical analysis

Data from research participants were analyzed using unpaired t-tests to compare general information, such as age. The chi-square test was used to analyze non-numeric data, such as gender. For the data from experimental animals, multiple repeated measures ANOVA with Bonferroni post hoc analysis was used to compare changes before and after the various values of the parameters. Additionally, Student's t-tests were conducted to compare groups of rats, and paired t-tests were employed to analyze data with normal distributed, paired measurements, while Wilcoxon matched pairs signed rank test was used to evaluate unequal distributed data such as urinary mineral excretion. In the gut microbiome analysis, the most abundant taxa at the phylum and genus levels were demonstrated at the ASV level. The Mann Whitney test was used to evaluate the relative bacterial species. The Kruskal-Wallis test was employed for alpha and beta diversity analysis. Statistical analyses were performed using SPSS version 23.0 (IBM Statistics, USA) and GraphPad Prism version 9.4 (DotMatics, USA). The statistically significant was obtained when $p < 0.05$. The Chi-square test was utilised to analyze the tissue results.

Results

Human urinary profile

Our study compared demographic and urinary biochemical parameters between control participants ($n = 10$) and people diagnosed with urolithiasis ($n = 8$) (Table 1). Demographic data, including gender distribution, age, and body mass index (BMI), did not show significant differences between the two groups. Participants with diabetes mellitus and hypertension were present in the urolithiasis group.

The urine biochemical analyses revealed significant disparities in several key parameters associated with the risk of stone. The calcium-to-creatinine ratio (Ca/Cr) and oxalate-to-creatinine ratio (Ox/Cr) were significantly elevated in the urolithiasis group compared to the control group. On the contrary, the citrate-to-creatinine ratio (Cit/Cr) was significantly reduced in the urolithiasis group. There was no significant difference in the magnesium-to-creatinine ratio (Mg/Cr) between the two groups. The pH tended to be lower in the urolithiasis group, although this did not reach statistical significance ($P = 0.097$). In particular, the urine supersaturation index, a marker of the risk of stone formation, was significantly higher in the urolithiasis group ($P = 0.027$).

Factors	Control ($n = 10$)	Urolithiasis ($n = 8$)	P-value
Participants information			
Gender (Male/Female)	3/7	2/6	0.060
Age (years)	43.5 ± 11.8	48.9 ± 14.6	0.449
Body mass index (kg/m ²)	24.826 ± 3.506	25.288 ± 3.526	0.785
Diabetes mellitus (persons)	0	1	
Hypertension (persons)	0	2	
Urinary parameters			
Ca/Cr (mg/gCr)	64.9 ± 43.7	257.3 ± 264.2*	0.043
Ox/Cr (mg/gCr)	20.9 ± 8.9	40.5 ± 11.7*	0.005
Cit/Cr (mg/gCr)	662.8 ± 266.1	355.2 ± 237.2*	0.031
Mg/Cr (mg/gCr)	174.7 ± 229.1	86.7 ± 53.8	0.573
Urine pH	6.8 ± 0.6	6.3 ± 0.7	0.097
Urine supersaturation index	25.7 ± 26.5	98.8 ± 102.2*	0.027

Table 1. Epidemiological data and urinary parameters of participants. Data expressed in mean ± SD, Ca: calcium, Cr: creatinine, Ox: oxalate, Cit: citrate, Mg: magnesium* $p < 0.05$ compared to healthy control.

Human microbiome study

There was no difference in alpha diversity between both groups, as shown in the Shannon index, richness, and evenness (Fig. 1). Similarly, beta-diversity did not show distinctive dissimilarity between healthy volunteers and urolithiasis patients.

For taxonomic analysis, the relative abundance of bacteria at the phylum levels is shown in Fig. 2. The increased relative abundance of *Bacteroidota* was found in patients with urolithiasis, while the abundance of other bacteria was not significantly different.

Comparative analysis of the human fecal microbiota, stratified by phylum, identified *Firmicutes* as the most prevalent phylum in both healthy control and urolithiasis cohorts. A noticeable decline in the relative abundance of the *Actinobacteriota* and *Proteobacteria* phyla was observed among individuals with urolithiasis. Furthermore, *Verrucomicrobiota* and *Desulfobacterota* phyla were consistently present in the fecal samples of both groups. Interestingly, at the genus level, *Bifidobacterium* and *Oscillospiraceae UCG002* were significantly depleted in the urolithiasis group compared to the healthy controls (supplementary Table S1).

Urinary parameters of rats transplanted with the fecal microbiota

Rats that received fecal microbiome transplants from healthy individuals did not show statistically significant changes in urinary excretion rates of calcium, oxalate and magnesium, nor in urine pH and urinary supersaturation index. The only change observed was a reduction in urinary citrate excretion, as illustrated in Fig. 3. On the contrary, rats that were transplanted with the fecal microbiota of patients with urolithiasis experienced an increase in both urine pH and urinary oxalate excretion rates, along with a decrease in urinary magnesium and citrate. In particular, the urinary supersaturation index showed a significant increase in these rats after FMT. Furthermore, the post-transplant urinary oxalate excretion rate in rats with the urolithiasis-derived microbiota exceeded that of their control counterparts.

Renal pathology and gene expression in animal tissues

Renal histopathological analysis revealed no evidence of tubular injury or calcium oxalate crystal deposition in either group, as shown in Fig. 4A. Expression of *NF-κB* mRNA in the renal tissues of urolithiasis-FMT rats

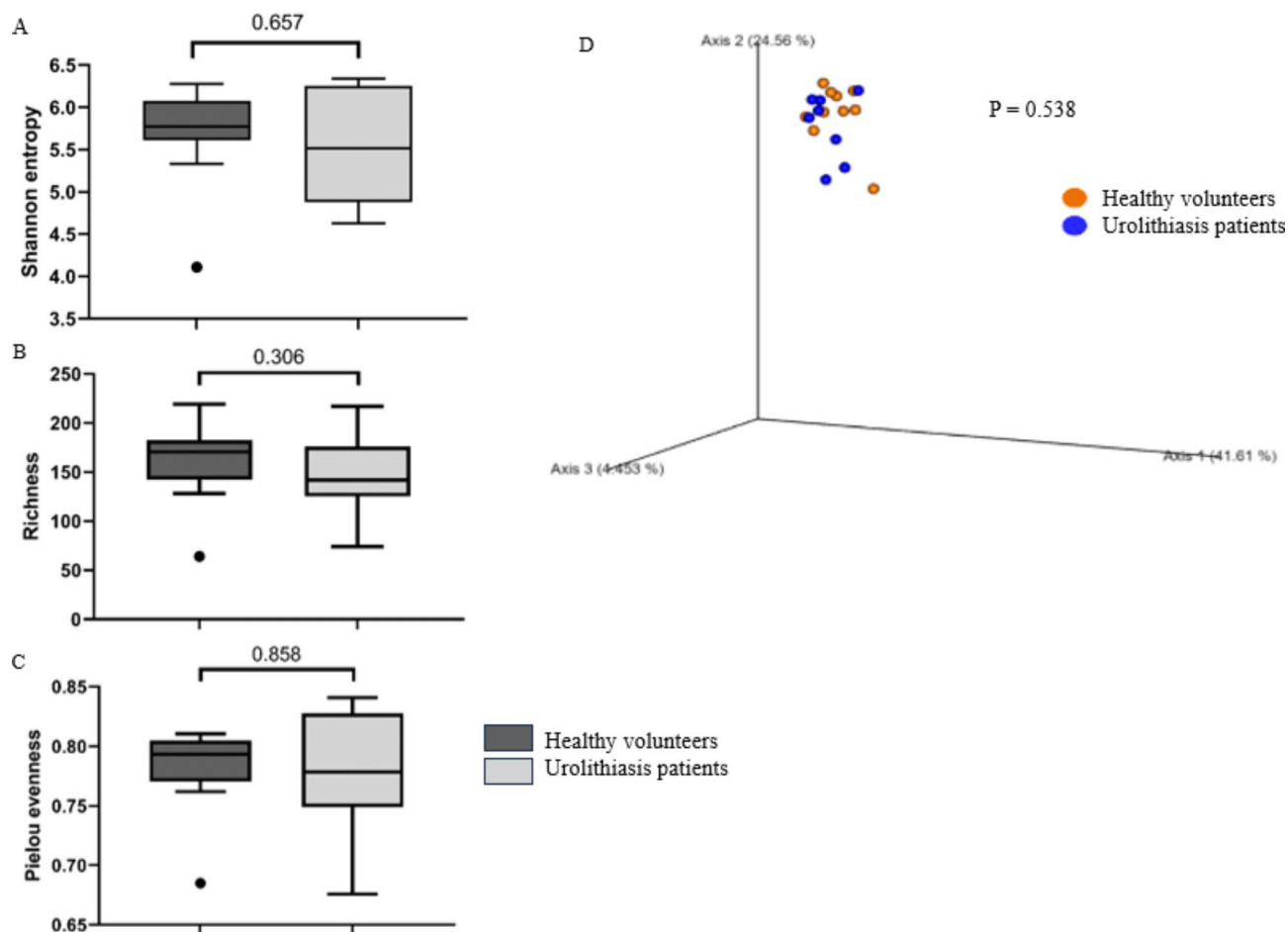


Fig. 1. The alpha and beta diversity of the fecal microbiota compared between healthy volunteers with human urolithiasis patients. No significant differences were detected in alpha-diversity (A) Shannon index, (B) richness, and (C) Evenness and (D) beta-diversity by PCoA based on Bray-Curtis dissimilarity index.

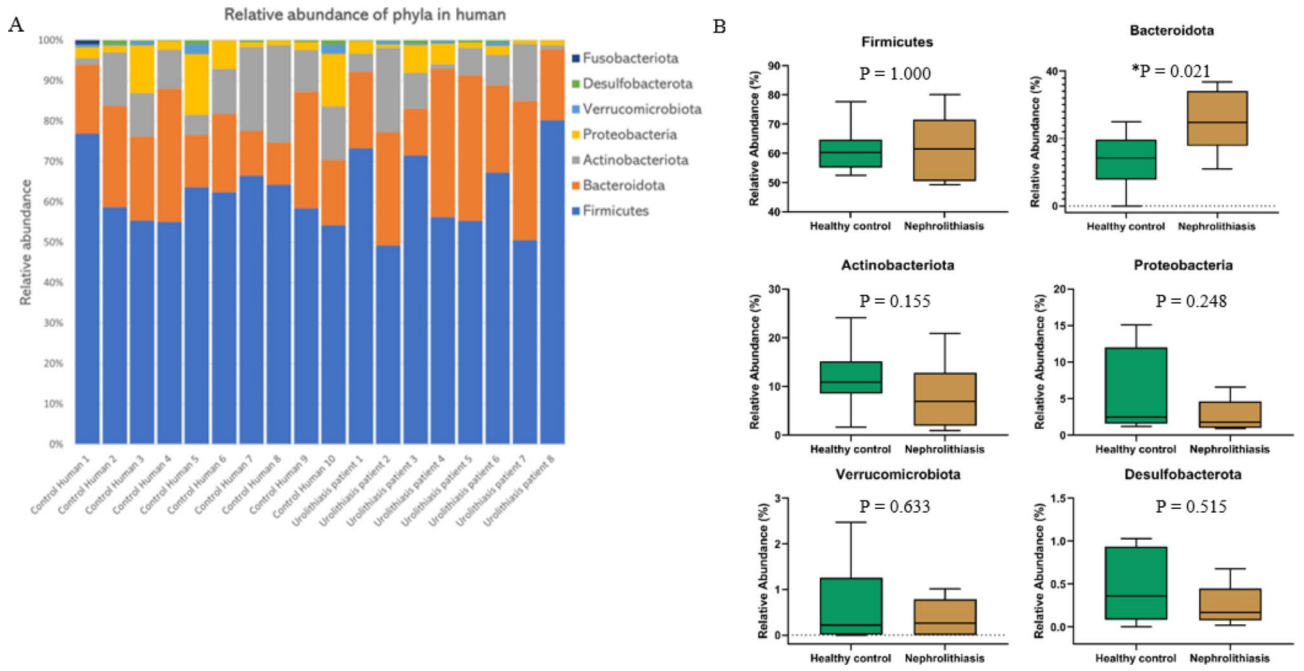


Fig. 2. Human fecal microbiome profile of healthy volunteer and urolithiasis patients. (A) The relative abundance of the most abundant microbiota in each subject. (B) Relative abundance of the human fecal microbiota in the phylum. * $p < 0.05$.

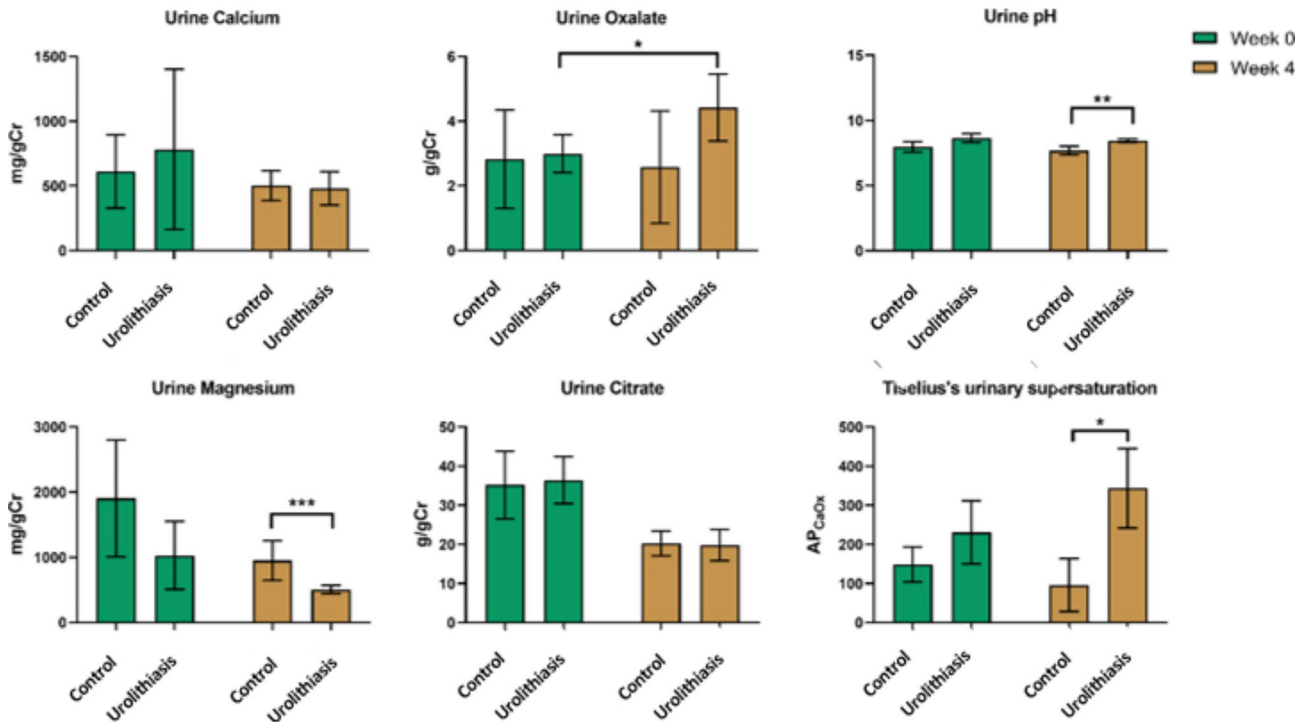


Fig. 3. The urinary parameters of the rats at week 0 and week 4 after fecal microbiota transplantation. Data were normalized by creatinine and presented as median \pm SD. Statistical significance was denoted as * $p < 0.05$, ** $p < 0.005$, and *** $p < 0.001$, compared to the control group.

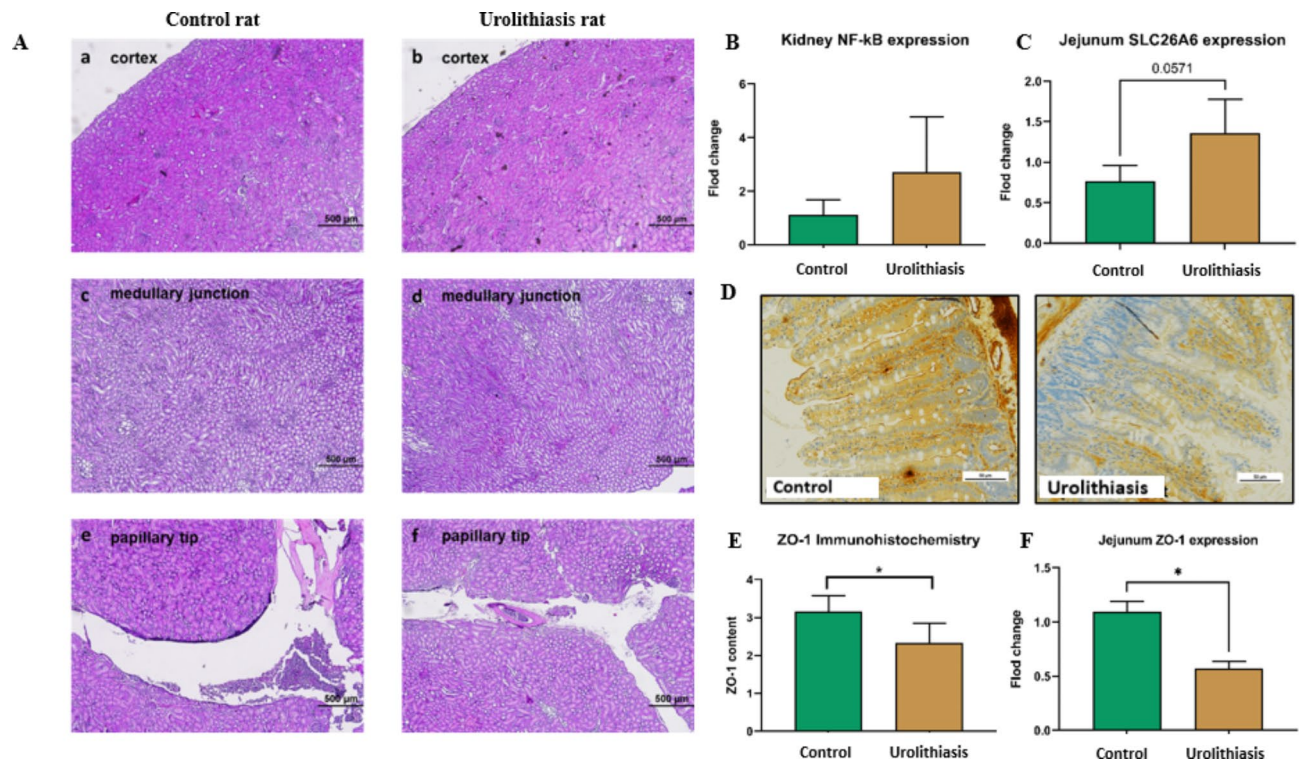


Fig. 4. The study of histopathology and gene expression in animal tissues. **(A)** Histopathological examination of the kidney under a polarized light microscope, categorized into control rats (a, c, and e) and urolithiasis rats (b, d, and f). **(B)** Analysis of *NF-kB* mRNA expression in kidney tissue. **(C)** Analysis of *SLC26A6* mRNA expression in jejunum tissue. **(D)** Histopathological examination of the jejunum using immunohistochemistry against ZO-1 (ZO-1 stained orange or brown, cytoplasm stained in blue) **(E)** Analysis of jejunal ZO-1 protein expression, and **(F)** Analysis of jejunal ZO-1 mRNA expression. Statistical significance was denoted as * $p < 0.05$ compared to the control group.

appeared to be nonstatistically significantly higher than healthy FMT rats, although non-statistical significance was obtained (Fig. 4B). In the intestines of FMT rats, there was an observed overexpression of *SLC26A6* mRNA (Fig. 4C). Furthermore, a down-regulation of ZO-1 protein expression detected by immunohistochemistry (Fig. 4D and E), and mRNA expression (Fig. 4F) were observed when compared to their control counterparts.

Animal microbiome study

Alpha diversity, measured using the Shannon index for control rats and urolithiasis rats after four weeks of FMT, showed an elevation in Shannon entropy for both groups. This suggests an increased richness and evenness of the bacterial population. However, a closer examination of alpha diversity at week 4 revealed that urolithiasis rats had a significantly lower relative abundance compared to control rats ($p < 0.05$). The comparison of beta diversity between pre- and post-FMT samples unveiled a statistically significant shift ($p < 0.01$), with an F value of 42.001 and R-squared of 0.683, indicative of significant compositional changes in the gut microbiota after FMT, as illustrated in Fig. 5A.

Phylum-level analysis of the pre-transplant fecal microbiota identified *Firmicutes* as the most populous phylum, as seen in Fig. 5B. In post-FMT, both groups exhibited a decrease in the relative abundance of *Firmicutes* compared to the initial measurements at week 0. At week 4, no significant difference in the relative abundance of *Firmicutes* ($p = 0.423$), but elevations of *Bacteroidota* were observed in urolithiasis rats ($p = 0.015$). However, a noteworthy decrease in *Euryarchaeota* ($p = 0.025$), coupled with increases in *Desulfobacterota* and *Cyanobacteria*, was observed in urolithiasis rats ($p = 0.010$ and 0.037 , respectively).

At the genus level, urolithiasis rats showed the increase in an abundance of *Muribaculaceae* (Phylum *Bacteroidota*) along with a decrease in *Prevotellaceae* (Phylum *Bacteroidota*), *Methanosphaera* (Phylum *Euryarchaeota*), *Roseburia*, *Colidextribacter* (Phylum *Bacillota*) and *Eubacterium siraeum*.

Discussion

Patients with urolithiasis in our study exhibited several known risk factors for stone formation, such as increased urinary excretion of calcium and oxalate coupled with reduced urinary citrate excretion. In particular, the urinary supersaturation index was significantly elevated, approximately 3.8 times higher in stones patients compared with healthy individuals, underscoring it as a critical risk factor for urolithiasis. Echoing previous research, our investigation also identified gut dysbiosis in patients with urolithiasis, characterized primarily by an increased abundance of *Bacteroidota*. This contrasts with previous reports that did not find significant changes in the

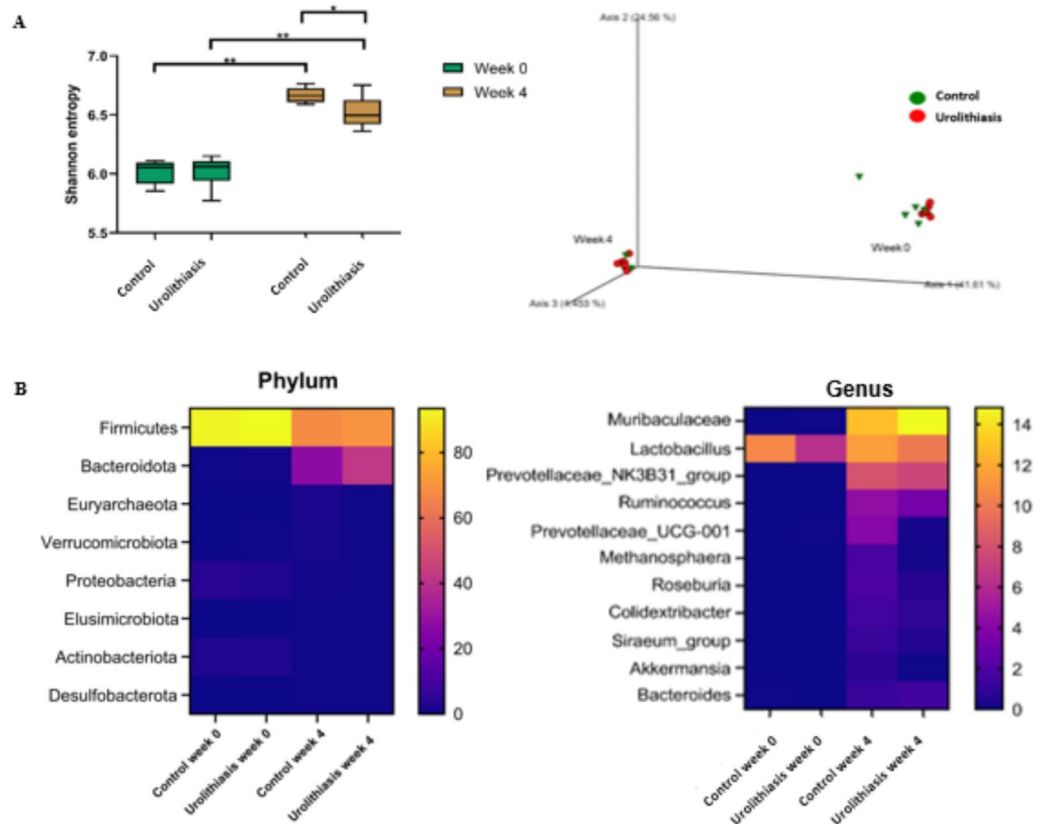


Fig. 5. The gut microbiome results in rats transplanted with the fecal microbiota. **(A)** alpha and beta diversity of pre- and post-fecal microbiota transplantation rats in each group; **(B)** The most abundant intestinal microbiota in each group was demonstrated in phylum and genus levels.

Escherichia_Shigella or *Prevotella*^{14,15}. Consistent increase in *Bacteroidota* abundance emerges as a hallmark of gut dysbiosis associated with urolithiasis.

Furthermore, we extended these findings to an animal model, where rats receiving fecal microbiota transplants from patients with urolithiasis also showed a higher prevalence of *Muribaculaceae* of the phylum *Bacteroidota* compared to those receiving transplants from healthy controls. This parallel increase in *Bacteroidota* suggests that fecal microbiota transplantation was effective in replicating the gut dysbiosis observed in human urolithiasis within the rat model. Our results support that gut dysbiosis could play a contributing role in the pathogenesis of urolithiasis and they affirm the potential of FMT as a tool to model disease-associated microbiota alterations in experimental settings.

In our study, urolithiasis-FMT rats later developed gut dysbiosis, exhibiting specific disorders that are recognized as risk factors for calcium oxalate urolithiasis. These included elevated urinary oxalate levels, decreased urinary magnesium, increased urine pH²⁶, and elevation of the urinary supersaturation index that was approximately three times higher compared to controls. These findings indicate the substantial influence of gut dysbiosis on the pathogenesis of urolithiasis, particularly implicating alterations in oxalate metabolism.

Oxalate in the body originates from two primary sources: dietary intake and endogenous synthesis. In the endogenous pathway, oxalate is a by-product of the metabolism of various biomolecules, including ascorbic acid, L-hydroxy-lysine, and glyoxalate²⁷. In our rat model, we maintained a consistent diet across the board, which should standardize the production of endogenous oxalate. However, the absorption of exogenous or dietary oxalate may differ significantly due to gut dysbiosis.

Gut dysbiosis is well established to lead to increased intestinal epithelial permeability²⁸, a process often linked to down-regulation of tight junction proteins, pro-inflammatory responses, endotoxin production, and bacterial translocation²⁹. Gram-negative bacteria proliferation in the gut, particularly *Bacteroides* spp., which constitutes the largest gram-negative phylum in the gut microbiota, correlates with increased endotoxins, especially lipopolysaccharides (LPS), thereby exacerbating gut permeability³⁰. Although some *Bacteroides* species produce less endotoxin or even inhibiting toxin production, the whole *Bacteroidota* phylum generates more endotoxin relative to other Gram-positive bacteria, such as *Firmicutes*^{31,32}. In this context, we hypothesized that the gut dysbiosis observed in urolithiasis could lead to compromised integrity of the intestinal barrier, enhancing the paracellular absorption of both LPS and oxalate. Our findings confirm this hypothesis, demonstrating that rats receiving FMT from urolithiasis patients not only exhibited gut dysbiosis but also showed reduced

expression of the intestinal tight junction protein ZO-1, indicative of potential gut leakage and could induce renal inflammation.

The chloride/oxalate transporter SLC26A6 is highly expressed in the renal epithelium, the apical regions of the salivary glands, and the villi of the small intestine, which spans from the duodenum through the jejunum and ileum, yet it is markedly reduced in the large intestine³³. The process of oxalate transport in the intestine is bidirectional, involving net absorption—primarily through transcellular (through the SLC26A1 and SLC26A3 transporters) and paracellular routes, and secretion, which is regulated by the SLC26A6 and, to a lesser extent, the SLC26A2 transporters³⁴. The role of intestinal SLC26A6 is pivotal in facilitating the clearance of serum oxalate, thus minimizing the oxalate load in body³⁵. Evidence from previous research indicates that wild-type mice with intact intestinal SLC26A6 expression exhibit resistance to urolithiasis³⁶, while SLC26A6 knockout (KO) mice are prone to hyperoxalemia, hyperoxaluria, and kidney stone³⁷. The expression of SLC26A6 is modulated by various factors, including inflammation, microRNAs, and metabolites. A study by Liu Y. in 2021 highlighted that short-chain fatty acids such as acetate and propionate improve intestinal SLC26A6 and reduced intestinal oxalate absorption²⁴. Recent research has shown that FMT rats with increased *Muribaculaceae*, *Lactobacillus*, and *Bifidobacterium* exhibited significantly lower urinary oxalate excretion and reduced calcium oxalate crystal deposition³⁸.

Our findings align with these observations, showing an up-regulation of intestinal SLC26A6 expression. This up-regulation can be attributed to a high influx of oxalate or the influence of an increased abundance of *Bacteroidota*, particularly *Muribaculaceae*, a prominent propionate-producing bacterial family^{39,40}. The increase in the intestinal oxalate-secreting transporter SLC26A6 could represent an adaptive mechanism to mitigate elevated serum oxalate levels resulting from enhanced intestinal absorption and intestinal leakage, thereby reducing the overall burden of oxalate burden in the body.

The limitations of this study are including the use of spot urine in the evaluation of urinary mineral excretion in volunteers and urolithiasis patients, which was less accurate, as the excretion of urinary calcium, oxalate, and citrate has a circadian pattern. We had minimized the fluctuation by collecting the morning first voiding urine from the participants. Secondly, germ-free rats are a better model for the microbiota transplantation model than antibiotic knockout rats. Residual native gut bacteria can potentially affect the proliferation and function of the transplanted microbiota. Lastly, we could not directly measure intestinal oxalate absorption due to free access to food and water from the animals, and the fecal oxalate content was not accurately measured, since the defecating interval of the rats was unexpected.

Conclusion

Our study reveals a notable link between the gut microbiota, dysbiosis, leaky gut syndrome, and urolithiasis. In particular, an increased abundance of *Bacteroidota* in patients with calcium oxalate stone disease is considered a risk factor for urolithiasis. This is because intestinal dysbiosis causes gut hyperpermeability, which stimulates intestinal oxalate absorption. This leads to hyperoxaluria and increased urinary supersaturation (Fig. 6). Furthermore, up-regulation of the SLC26A6 transporter in the context of urolithiasis underscores potential compensatory responses to increased oxalate levels, possibly influenced by the prevalence of *Muribaculaceae*. Addressing intestinal dysbiosis emerges as a strategic consideration to mitigate urolithiasis in high-risk individuals.

Declaration of AI and AI-assisted technologies in the writing process

In the development of this manuscript, the author employed Writefull for grammatical corrections, and BioRender.com to create a figure. Following the utilization of this tool, the author meticulously reviewed and adjusted the content where necessary, assuming complete accountability for the final submission.

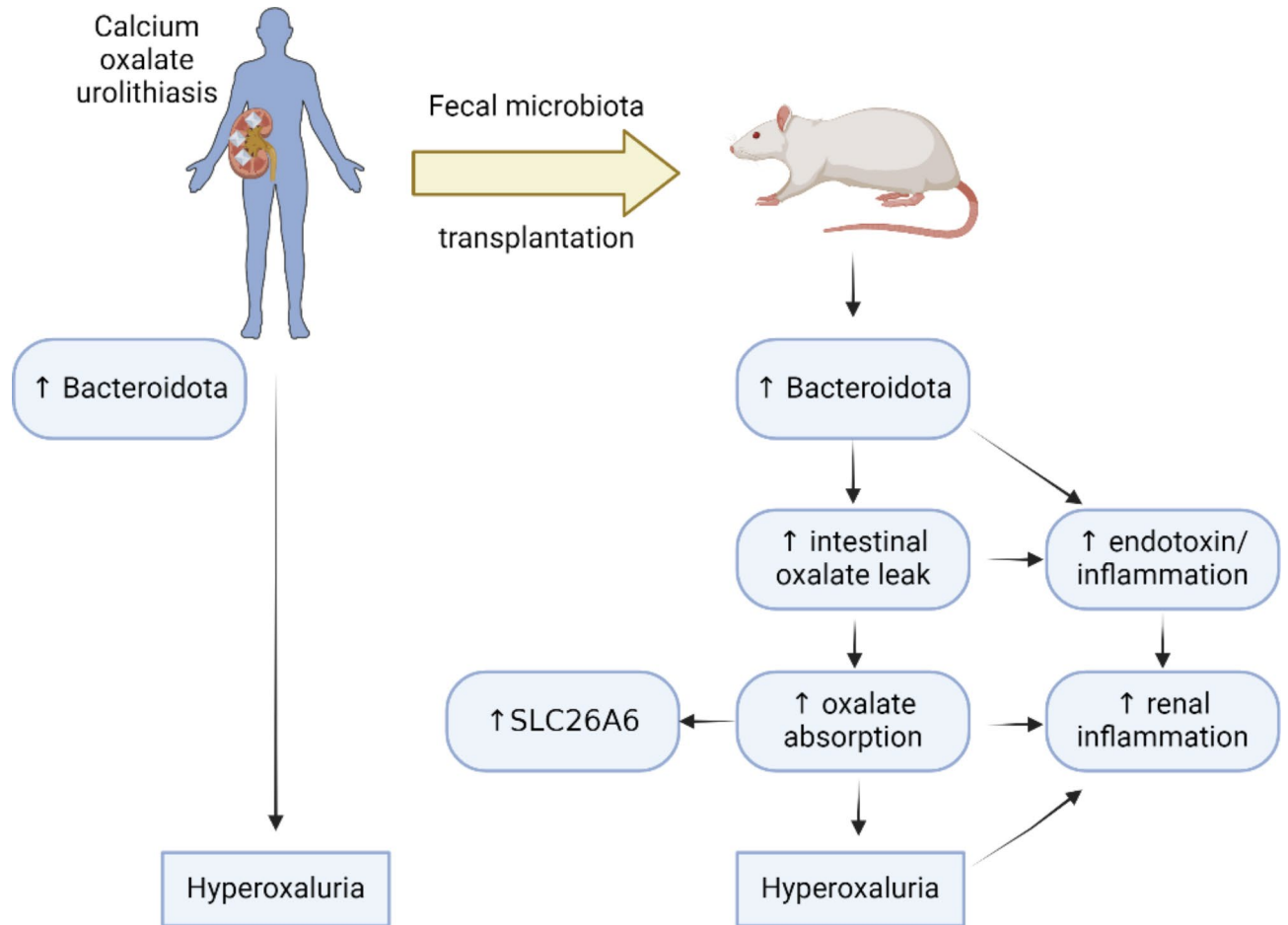


Fig. 6. The hypothesis of gut *Bacteroidota* overabundance in calcium oxalate urolithiasis, created with BioRender.com.

Data availability

The 16 S rRNA sequences of fecal from humans and rats generated and/or analysed during the current study are available in the NCBI BioProject repository, ID PRJNA1139982.

Received: 20 March 2024; Accepted: 10 September 2024

Published online: 20 September 2024

References

1. Tzelves, L., Türk, C. & Skolarikos, A. European association of urology urolithiasis guidelines: Where are we going? *Eur. Urol. Focus* **7**, 34–38. <https://doi.org/10.1016/j.euf.2020.09.011> (2021).
2. Li, S. et al. Trends in the incidence and DALYs of urolithiasis from 1990 to 2019: Results from the global burden of disease study 2019. *Front. Public Health* **10**, 825541. <https://doi.org/10.3389/fpubh.2022.825541> (2022).
3. Xu, Z., Yao, X., Duan, C., Liu, H. & Xu, H. Metabolic changes in kidney stone disease. *Front. Immunol.* **14**, 1142207. <https://doi.org/10.3389/fimmu.2023.1142207> (2023).
4. Crivelli, J. J. et al. Contribution of dietary oxalate and oxalate precursors to urinary oxalate excretion. *Nutrients* <https://doi.org/10.3390/nu13010062> (2020).
5. Pence, S. et al. Low *Oxalobacter formigenes* colonization is associated with reduced bone mineral density in urinary stone forming patients. *Curr. Urol.* **8**, 189–193. <https://doi.org/10.1159/000365715> (2015).
6. Batislam, E., Yilmaz, E., Yuvanc, E., Kisa, O. & Kisa, U. Quantitative analysis of colonization with real-time PCR to identify the role of oxalobacter formigenes in calcium oxalate urolithiasis. *Urol. Res.* **40**, 455–460. <https://doi.org/10.1007/s00240-011-0449-8> (2012).
7. Verhulst, A., Dehmel, B., Lindner, E., Akerman, M. E. & D'Haese, P. C. *Oxalobacter formigenes* treatment confers protective effects in a rat model of primary hyperoxaluria by preventing renal calcium oxalate deposition. *Urolithiasis* **50**, 119–130. <https://doi.org/10.1007/s00240-022-01310-9> (2022).
8. Chmiel, J. A. et al. New perspectives on an old grouping: The genomic and phenotypic variability of *Oxalobacter formigenes* and the implications for calcium oxalate stone prevention. *Front. Microbiol.* **13**, 1011102. <https://doi.org/10.3389/fmicb.2022.1011102> (2022).
9. Kachroo, N. et al. Meta-analysis of clinical microbiome studies in urolithiasis reveal age, stone composition, and study location as the predominant factors in urolithiasis-associated microbiome composition. *mBio* **12**, e0200721. <https://doi.org/10.1128/mBio.02007-21> (2021).

10. Ariceta, G. et al. ePHex: A phase 3, double-blind, placebo-controlled, randomized study to evaluate long-term efficacy and safety of *Oxalobacter formigenes* in patients with primary hyperoxaluria. *Pediatr. Nephrol.***38**, 403–415. <https://doi.org/10.1007/s00467-022-05591-5> (2023).
11. Miller, A. W. & Dearing, D. The metabolic and ecological interactions of oxalate-degrading bacteria in the mammalian gut. *Pathogens***2**, 636–652. <https://doi.org/10.3390/pathogens2040636> (2013).
12. Wigner, P., Bijak, M. & Saluk-Bijak, J. Probiotics in the prevention of the calcium oxalate urolithiasis. *Cells* (2022). <https://doi.org/10.3390/cells11020284>
13. Stern, J. M. et al. Evidence for a distinct gut microbiome in kidney stone formers compared to non-stone formers. *Urolithiasis***44**, 399–407. <https://doi.org/10.1007/s00240-016-0882-9> (2016).
14. Yuan, T. et al. Gut microbiota in patients with kidney stones: A systematic review and meta-analysis. *BMC Microbiol.***23**, 143. <https://doi.org/10.1186/s12866-023-02891-0> (2023).
15. Stern, J. M. et al. Fecal transplant modifies urine chemistry risk factors for urinary stone disease. *Physiol. Rep.***7**, e14012. <https://doi.org/10.14814/phy2.14012> (2019).
16. Tiselius, H. G. Aspects on estimation of the risk of calcium oxalate crystallization in urine. *Urol. Int.***47**, 255–259. <https://doi.org/10.1159/000282232> (1991).
17. Bokoliya, S. C., Dorsett, Y., Panier, H. & Zhou, Y. Procedures for fecal microbiota transplantation in murine microbiome studies. *Front. Cell. Infect. Microbiol.***11**, 711055. <https://doi.org/10.3389/fcimb.2021.711055> (2021).
18. Ma, S., Wang, N., Zhang, P., Wu, W. & Fu, L. Fecal microbiota transplantation mitigates bone loss by improving gut microbiome composition and gut barrier function in aged rats. *PeerJ***9**, e12293. <https://doi.org/10.7717/peerj.12293> (2021).
19. Schmidt, E. K. A. et al. Fecal transplant prevents gut dysbiosis and anxiety-like behaviour after spinal cord injury in rats. *PLoS One***15**, e0226128. <https://doi.org/10.1371/journal.pone.0226128> (2020).
20. Tiselius, H. G., Ferraz, R. R. & Heilberg, I. P. An approximate estimate of the ion-activity product of calcium oxalate in rat urine. *Urol. Res.***31**, 410–413. <https://doi.org/10.1007/s00240-003-0363-9> (2003).
21. Yamaguchi, S. et al. Study of a rat model for calcium oxalate crystal formation without severe renal damage in selected conditions. *Int. J. Urol.***12**, 290–298. <https://doi.org/10.1111/j.1442-2042.2005.01038.x> (2005).
22. Vaziri, N. D. et al. Disintegration of colonic epithelial tight junction in uremia: A likely cause of CKD-associated inflammation. *Nephrol. Dial. Transpl.***27**, 2686–2693. <https://doi.org/10.1093/ndt/gfr624> (2012).
23. Li, H. et al. Increased oxidative stress and disrupted small intestinal tight junctions in cigarette smoke-exposed rats. *Mol. Med. Rep.***11**, 4639–4644. <https://doi.org/10.3892/mmr.2015.3234> (2015).
24. Liu, Y. et al. Short-chain fatty acids reduced renal calcium oxalate stones by regulating the expression of intestinal oxalate transporter SLC26A6. *mSystems***6**, e0104521. <https://doi.org/10.1128/mSystems.01045-21> (2021).
25. Miri, S., Rasooli, A. & Brar, S. K. Data on changes of NF- κ B gene expression in liver and lungs as a biomarker and hepatic injury in CLP-induced septic rats. *Data Brief***25**, 104117. <https://doi.org/10.1016/j.dib.2019.104117> (2019).
26. Gombedza, F. C., Shin, S., Sadiua, J., Stackhouse, G. B. & Bandyopadhyay, B. C. The rise in tubular pH during hypercalciuria exacerbates calcium stone formation. *Int. J. Mol. Sci.* <https://doi.org/10.3390/ijms25094787> (2024).
27. Baltazar, P. et al. Oxalate (dys)metabolism: Person-to-person variability, kidney and cardiometabolic toxicity. *Genes (Basel)*. <https://doi.org/10.3390/genes14091719> (2023).
28. Allam-Ndoul, B., Castonguay-Paradis, S. & Veilleux, A. Gut microbiota and intestinal trans-epithelial permeability. *Int. J. Mol. Sci.* <https://doi.org/10.3390/ijms21176402> (2020).
29. Mishra, S. P. et al. A mechanism by which gut microbiota elevates permeability and inflammation in obese/diabetic mice and human gut. *Gut*. <https://doi.org/10.1136/gutjnl-2022-327365> (2023).
30. Lukiw, W. J. *Bacteroides fragilis* lipopolysaccharide and inflammatory signaling in Alzheimer's disease. *Front. Microbiol.***7**, 1544. <https://doi.org/10.3389/fmicb.2016.01544> (2016).
31. Yoshida, N. et al. A possible beneficial effect of *Bacteroides* on faecal lipopolysaccharide activity and cardiovascular diseases. *Sci. Rep.***10**, 13009. <https://doi.org/10.1038/s41598-020-69983-z> (2020).
32. Fei, N. et al. Endotoxin producers overgrowing in human gut microbiota as the causative agents for nonalcoholic fatty liver disease. *mBio* (2020). <https://doi.org/10.1128/mBio.03263-19>
33. Wang, Z. et al. Renal and intestinal transport defects in Slc26a6-null mice. *Am. J. Physiol. Cell. Physiol.***288**, C957–965. <https://doi.org/10.1152/ajpcell.00505.2004> (2005).
34. Wang, J., Wang, W., Wang, H. & Tuo, B. Physiological and pathological functions of SLC26A6. *Front. Med. (Lausanne)***7**, 618256. <https://doi.org/10.3389/fmed.2020.618256> (2020).
35. Neumeier, L. I. et al. Enteric oxalate secretion mediated by Slc26a6 defends against hyperoxalemia in murine models of chronic kidney disease. *J. Am. Soc. Nephrol.***31**, 1987–1995. <https://doi.org/10.1681/asn.2020010105> (2020).
36. Soleimani, M. The role of SLC26A6-mediated chloride/oxalate exchange in causing susceptibility to nephrolithiasis. *J. Physiol.***586**, 1205–1206. <https://doi.org/10.1113/jphysiol.2007.150565> (2008).
37. Jiang, Z. et al. Calcium oxalate urolithiasis in mice lacking anion transporter Slc26a6. *Nat. Genet.***38**, 474–478. <https://doi.org/10.1038/ng1762> (2006).
38. Wang, Y. et al. Increased abundance of bacteria of the family Muribaculaceae achieved by fecal microbiome transplantation correlates with the inhibition of kidney calcium oxalate stone deposition in experimental rats. *Front. Cell. Infect. Microbiol.***13**, 1145196. <https://doi.org/10.3389/fcimb.2023.1145196> (2023).
39. Parada Venegas, D. et al. Short chain fatty acids (SCFAs)-mediated gut epithelial and immune regulation and its relevance for inflammatory bowel diseases. *Front. Immunol.***10**, 277. <https://doi.org/10.3389/fimmu.2019.00277> (2019).
40. Smith, B. J. et al. Changes in the gut microbiome and fermentation products concurrent with enhanced longevity in acarbose-treated mice. *BMC Microbiol.***19**, 130. <https://doi.org/10.1186/s12866-019-1494-7> (2019).

Acknowledgements

This research was funded by the Ratchadapiseksompotch Fund, Faculty of Medicine, Chulalongkorn University, grant number RA65/045 and the Program Management Unit for Human Resources and Institutional Development, Research, and Innovation (PMU-B), grant number B36G660010. We would like to thank Miss Panumas Kamkeng, Miss Tanyaporn Keratibumrunpong, and Mr. Tawatchai Chumponsuk of Metabolic Disease in Gastrointestinal and Urinary System Research Unit, staff of Center of Excellence in Hepatitis and Liver Cancer, Department of Biochemistry, and staff of the Animal Center, Faculty of Medicine, Chulalongkorn University and ModGut Co.Ltd for their generous help.

Author contributions

T.D. Conceptualization; M.U., M.S., T.D. Methodology; S.H., Validation; S.H., N.C., T.D. Formal analysis; S.H., W.A., M.T., T.D. Investigation; M.U., T.D. Resources; S.H. Data curation; S.H. Writing original draft preparation; T.D. Review and editing; S.H., N.C., T.D. Visualization; M.U., M.S., P.T., P.R., N.C., T.D. Supervision. T.D. Project administration; T.D. Funding acquisition. All authors reviewed the manuscript.

Declarations

Competing interests

The authors declare no competing interests.

Additional information

Supplementary Information The online version contains supplementary material available at <https://doi.org/10.1038/s41598-024-72694-4>.

Correspondence and requests for materials should be addressed to T.D.

Reprints and permissions information is available at www.nature.com/reprints.

Publisher's note Springer Nature remains neutral with regard to jurisdictional claims in published maps and institutional affiliations.

Open Access This article is licensed under a Creative Commons Attribution-NonCommercial-NoDerivatives 4.0 International License, which permits any non-commercial use, sharing, distribution and reproduction in any medium or format, as long as you give appropriate credit to the original author(s) and the source, provide a link to the Creative Commons licence, and indicate if you modified the licensed material. You do not have permission under this licence to share adapted material derived from this article or parts of it. The images or other third party material in this article are included in the article's Creative Commons licence, unless indicated otherwise in a credit line to the material. If material is not included in the article's Creative Commons licence and your intended use is not permitted by statutory regulation or exceeds the permitted use, you will need to obtain permission directly from the copyright holder. To view a copy of this licence, visit <http://creativecommons.org/licenses/by-nc-nd/4.0/>.

© The Author(s) 2024, corrected publication 2024